BRILL

Multidiscipline Modeling in Mat. and Str.5(2009)119-138

MMMS
www.brill.nl/mmms

REFINED MULTILAYERED PLATE ELEMENTS FOR COUPLED MAGNETO-ELECTRO-ELASTIC ANALYSIS

Carrera E[1], Di Gifico M, Nali P, Brischetto S
Aeronautics and Space Engineering Department, Politecnico di Torino, Turin, Italy
[1]Professor of Aerospace Structures and Applied Aeroelasticity, Aeronautics and space Engineering Department, Politecnico di Torino, Corso Duca degli Abruzzi, 24,10129 Torino, ITALY,
tel +39.011.564.6836, fax +39.011.564.6899
erasmo.carrera@polito.it

Received 5 June 2007; accepted 8 September 2007

Abstract

Finite elements for the analysis of multilayered plates subjected to magneto-electro-elastic fields are developed in this work. An accurate description of the various field variables has been provided by employing a variable kinematic model which is based on the Unified Formulation, UF. Displacements, magnetic and electric potential have been chosen as independent unknowns. Equivalent single layer and layer-wise descriptions have been accounted for. Plate models with linear up to fourth-order distribution in the thickness direction have been compared. The extension of the principle of virtual displacements to magneto-electro-elastic continua has been employed to derive finite elements governing equations. According to UF these equations are presented in terms of fundamental nuclei whose form is not affected by kinematic assumptions. Results show the effectiveness of the proposed elements as well as their capability, by choosing appropriate kinematics, to accurately trace the static response of laminated plates subject to magneto-electro-elastic fields.

Keywords
Finite Elements, Multilayered Plates, Magneto-electro-elastic problems, Refined Models, Smart Structures

1. Introduction

The introduction of non conventional materials has always played a key-role in the design and construction of lighter and more performant vehicles. About 80 years ago, in fact, the use of aluminum alloys has permitted to build first generation modern aircraft. Further, in the late sixties, the advent of composite materials (we refer to those reinforced by carbon/glass-fibers) has lead to the construction of the most efficient helicopters, fighters, ultra-light, glider and unmanned aircraft. Benefits of these applications have often been extended to automotive and ship vehicles as well as to civil engineering constructions. According to that historical trend, it is worldwide taught that the development of next generation vehicles is very much subordinate to the capability of using so called intelligent systems which make large use of smart structures. These structures are mostly characterized by the use of piezo-electric and/or piezo-magnetic materials that can be used as both sensors and actuators to make a closed loop control 'smart' structure, see [1], [2]. Sensors and actuators are obtained by coupling the mechanical, electrical and magnetic fields acting on the structures via so-called inverse or direct effects [3], [4] and [5]. For instance, mechanical strains are measured on piezoelectric materials (PEMs) if an electrical field is applied, vice-versa an electrical charge is obtained if mechanical loadings are applied to a piezoelectric made structure. The same happens if magnetical/electrical fields (actuator cases) or mechanical loadings (sensor cases) are applied to a structure made by magneto-electro-elastic materials (MEEMs).

In the applications, both PEMs and MEEMs are embedded as patches or, more conveniently, as embedded layers in multilayered structures (MLS) which are often made by composite materials. The study of smart systems therefore involves the analysis of MLS (often with anisotropic behaviors) under a combined action of multifield loadings (multifield problems MFP), see [6]. A number of requirements must be taken into account for an accurate analysis of MFP and MLS. The following points are herein of interest:

1. Constitutive equations must be derived in a consistent form.
2. Coupling among the various fields should be accurately described.
3. Inter-layer continuity of relevant variables must be guaranteed.
4. Employed kinematic models must be rich enough to describe the localized trough-the-thickness-distribution of involved fields in the various layers.

Reference to thermodynamic basis is mandatory for what at point 1, see [5].

Concerning point 2, the coupling could be introduced in a *partial* or *full* form. When the coupling is partial, constitutive laws are un-coupled and the effect of coupling is only introduced as an external loading. If the coupling is fully introduced, the used constitutive relations are coupled. For instance, if the magneto-elastic coupling is fully included in the formulation, the magneto-elastic stiffness appears in the governing equations.

As far as point 3 is concerned, it is known that a classical choice for the primary variables for the various fields could violate some physical relations. This is the case of transverse shear and normal stresses which for equilibrium reasons must be continuous at each layer interface. Such a continuity is not enforced in usual models that make use of only displacement variables [7]. The same could be said for transverse electrical displacements, heat flux or transverse magnetical inductance [8], [9].

As at point 4, the use of variable (trough the thickness) kinematic models is mandatory in MLS subjected to MFP loadings. These loadings, in fact, have a *isotropic/anisotropic* and *localized* nature. Loadings coming from these fields are completely different from those for mechanical cases. As a consequence those kinematical models that were originally proposed for plate and shell structures subjected to mechanical loadings could show difficulties to analyze MFP. Modelings that permit the use of both Equivalent Single Layer Models, ESLM (the multilayered plate is seen as an equivalent one-layered plate), and Layer Wise Models, LWM models (the variables are independent in each layer) are mandatory in that case. A complete overview of variational statements for MFP and MLS has been recently given by Carrera et al. [6].

Among the possible multifield problems this paper restricts the attention to the MEEMs analysis of laminated plates. Applications of MEEMs have been made in ultrasonic imaging devices, sensors, actuators, transducers and other emerging components including plasma jets for fluid control applications [10]. Studies on static and dynamic behaviour of MEEMs made structures have been dealt in the recent literature. A review is given in the following. Pan [11] derived an exact closed-form solution for the simply supported and multilayered plate made of anisotropic piezoelectric and piezo-magnetic materials under static mechanical loads. Pan and Heyliger [12] solved the corresponding vibration problem. The behaviour of infinitely long cylindrical shells under uniform internal pressure has been studied by Wang and Zhong [13] and they conclude that piezoelectric and piezo-magnetic composites in general have the coupling effect which is two orders higher than that of single-phase magnetoelectric constituent materials; such a coupling cannot be discarded in the analyses. Micro-mechanical analysis of fully coupled electro-magneto-thermo-elastic composites has been carried out by Aboudi [14] for the prediction of the effective moduli of magneto-electro-elastic composites. From the literature survey, it is found that only few studies have been reported on magneto-electro-elastic structures by finite element analysis. Free vibration behaviour of infinitely long magneto-electro-elastic cylindrical shell has been studied by Buchanan [15] by using semi-analytical finite element method. The same author [16] has studied the behaviour of layered versus multiphase magneto-electro-elastic infinite long composite plate by finite element method. Wang et al [17] derived the state vector approach for the analysis of multilayered magneto-electro-elastic plates for mechanical and electrical loading. Lage et al. [18] developed a layerwise partial mixed finite element model for magneto-electro-elastic plate. The studies on non-homogeneous magneto-electro-elastic structure are less in the literature. Chen and Lee [19] adopted a state space formulation to derive equations for non-homogeneous transversely isotropic magneto-electro-elastic plates. Results on vibration have been considered in [20]. Chen et al. [21] have used state-vector approach to modal analysis of MEE plates. A theoretical contribution to modelling of linearly MEE thin plates has been given by Weller and Licht [22].

The present work proposes a variable kinematic finite element model which is based on Unified Formulation (UF) by extending previous authors' findings [9], [23], [24], [25], [26] and [27]. What at points 1, 2 and 4, they are fully addressed in the present work. The extended Principle of Virtual Displacements (PVD) to MEE continua is used to derive fundamental nuclei of couple magneto-electric-elastic problems. Displacements, electric and magnetic potential are assumed at layer or multilayer level, by leading to the so called layer-wise (LW) and equivalent single layer (ESL) description, respectively. The order of the expansion in the thickness layer/plate directions varies from linear to fourth order. As a result classical, higher order and layer-wise plates elements are formulated to evaluate the static response of layered plates embedding piezo-magnetic layers. The paper has been organized as it follows. Sec.2 gives constitutive and geometrical relations. Extension of PVD to MEE continua is given in Sec.3. Unified formulation for the considered plate elements is presented in Sec.4. Fundamental nuclei of finite element matrices and assessments and results for static bending problems are discussed in Sec.4.3. The Appendix quotes the explicit form of the obtained fundamental nuclei.

2. Preliminary

The geometry and the coordinate system of the laminated plate with N_l layers, has been represented in Fig. 1, including the MEE-layers. The reference system is denoted by x . y and z ; the correspondent plate dimensions are denoted by the letter a, b and h, respectivaly. The latter coordinate denotes the thickness direction. The number 1, 2 and 3 will be used in case of the material reference system.

2.1 Constitutive MEE equations

Material properties of a magneto-electro-elastic continua can be expressed in various forms. The so called e -forms [5] is considered in this work. The related energy coincides to the Electric energy G_2, which takes the following form:

$$G_2 = \frac{1}{2}\varepsilon^T \mathbf{C}^{E,H}\varepsilon - \mathbf{E}^T\mathbf{e}^{\mathbf{H}}\varepsilon - \frac{1}{2}\mathbf{E}^T\varepsilon^{\varepsilon,H}\mathbf{E} - \frac{1}{2}\mathbf{H}^T\mu^{\varepsilon,E}\mathbf{H} - \varepsilon^T\mathbf{q}^{\mathbf{E}}\mathbf{H} - \mathbf{E}^T\mathbf{d}^{\varepsilon}\mathbf{H}. \quad (1)$$

Where ε is the strain vector, $\mathbf{E}$ is the electric field vector, $\mathbf{H}$ is the magnetic field vector, $\mathbf{C}^{E,H}$ is the stiffness matrix calculated at constant E, H, $\mathbf{e}^H$ is the piezoelectric matrix which couples electrical and mechanical fields calculated at constant E, $\mathbf{q}^E$ is the piezo-magnetic matrix which couples magnetic and mechanical fields, $\varepsilon^{\varepsilon,H}$ is the permittivity matrix calculated at constant ε, H , $\mu^{\varepsilon,E}$ is the permittivity matrix calculated at constant ε, E and d^{ε} is the magnetoelectric matrix calculated at constant ε. The superscript T denotes the transposed matrices. The coefficients of the introduced matrices are obtained by the Magneto-Electric Gibbs energy according to the following derivatives:

$$\varepsilon_{mn}^{\varepsilon,H} = -\frac{\partial^2 G_2}{\partial E_m \partial E_n},\; e_{nij}^{H} = -\frac{\partial^2 G_2}{\partial E_n \partial \varepsilon_{ij}},\; C_{ijkl}^{E,H} = \frac{\partial^2 G_2}{\partial \varepsilon_{kl}\partial \varepsilon_{ij}} \quad (2)$$

$$\mu_{mn}^{\varepsilon,E} = -\frac{\partial^2 G_2}{\partial H_m \partial H_n},\; q_{nij}^{E} = -\frac{\partial^2 G_2}{\partial H_n \partial \varepsilon_{ij}},\; d_{nm}^{\varepsilon} = -\frac{\partial^2 G_2}{\partial H_n \partial E_m} \quad (3)$$

The stress vector σ, the electric displacement vector $\mathbf{D}$ and the magnetic inductance vector $\mathbf{B}$ can be obtained from Eq.(1), as in the following:

$$\sigma = \frac{\partial G_2}{\partial \varepsilon},\; \mathbf{D} = -\frac{\partial G_2}{\partial \mathbf{E}},\; \mathbf{B} = -\frac{\partial G_2}{\partial \mathbf{H}} \quad (4)$$

The following set of constitutive equations, related to the *k*-th layer are obtained:

$$\begin{aligned} \sigma^k &= \mathbf{C}^k\,\varepsilon^k - \mathbf{e}^{kT}\,\mathbf{E}^k - \mathbf{q}^{kT}\,\mathbf{H}^k \\ \mathbf{D}^k &= \mathbf{e}^k\,\varepsilon^k + \varepsilon^k\,\mathbf{E}^k + \mathbf{d}^k\,\mathbf{H}^k \\ \mathbf{B}^k &= \mathbf{q}^k\,\varepsilon^k + \mathbf{d}^k\,\mathbf{E}^k + \mu^k\,\mathbf{H}^k \end{aligned} \quad (5)$$

The explicit form of the introduced arrays, written in the material reference system 1-2-3, are:

$$\begin{bmatrix}\sigma_1\\\sigma_2\\\sigma_3\\\sigma_4\\\sigma_5\\\sigma_6\end{bmatrix}^k=\begin{bmatrix}C_{11}&C_{12}&C_{13}&0&0&C_{16}\\C_{12}&C_{22}&C_{23}&0&0&C_{26}\\C_{13}&C_{23}&C_{33}&0&0&C_{36}\\0&0&0&C_{44}&C_{45}&0\\0&0&0&C_{45}&C_{55}&0\\C_{16}&C_{26}&C_{36}&0&0&C_{66}\end{bmatrix}^k\begin{bmatrix}\varepsilon_1\\\varepsilon_2\\\varepsilon_3\\\varepsilon_4\\\varepsilon_5\\\varepsilon_6\end{bmatrix}^k$$
$$-\begin{bmatrix}0&0&e_{31}\\0&0&e_{32}\\0&0&e_{33}\\e_{14}&e_{24}&0\\e_{15}&e_{25}&0\\0&0&e_{36}\end{bmatrix}^k\begin{bmatrix}E_1\\E_2\\E_3\end{bmatrix}^k-\begin{bmatrix}0&0&q_{31}\\0&0&q_{32}\\0&0&q_{33}\\q_{14}&q_{24}&0\\q_{15}&q_{25}&0\\0&0&q_{36}\end{bmatrix}^k\begin{bmatrix}H_1\\H_2\\H_3\end{bmatrix}^k \tag{6}$$

$$\begin{bmatrix}D_1\\D_2\\D_3\end{bmatrix}^k=\begin{bmatrix}0&0&0&e_{14}&e_{15}&0\\0&0&0&e_{24}&e_{25}&0\\e_{31}&e_{32}&e_{33}&0&0&e_{36}\end{bmatrix}^k\begin{bmatrix}\varepsilon_1\\\varepsilon_2\\\varepsilon_3\\\varepsilon_4\\\varepsilon_5\\\varepsilon_6\end{bmatrix}^k$$
$$+\begin{bmatrix}\varepsilon_{11}&\varepsilon_{12}&0\\\varepsilon_{12}&\varepsilon_{22}&0\\0&0&\varepsilon_{33}\end{bmatrix}^k\begin{bmatrix}E_1\\E_2\\E_3\end{bmatrix}^k+\begin{bmatrix}d_{11}&d_{12}&0\\d_{12}&d_{22}&0\\0&0&d_{33}\end{bmatrix}^k\begin{bmatrix}H_1\\H_2\\H_3\end{bmatrix}^k \tag{7}$$

$$\begin{bmatrix}B_1\\B_2\\B_3\end{bmatrix}^k=\begin{bmatrix}0&0&0&q_{14}&q_{15}&0\\0&0&0&q_{24}&q_{25}&0\\q_{31}&q_{32}&q_{33}&0&0&q_{36}\end{bmatrix}^k\begin{bmatrix}\varepsilon_1\\\varepsilon_2\\\varepsilon_3\\\varepsilon_4\\\varepsilon_5\\\varepsilon_6\end{bmatrix}^k$$
$$+\begin{bmatrix}d_{11}&d_{12}&0\\d_{12}&d_{22}&0\\0&0&d_{33}\end{bmatrix}^k\begin{bmatrix}E_1\\E_2\\E_3\end{bmatrix}^k+\begin{bmatrix}\mu_{11}&\mu_{12}&0\\\mu_{12}&\mu_{22}&0\\0&0&\mu_{33}\end{bmatrix}^k\begin{bmatrix}H_1\\H_2\\H_3\end{bmatrix}^k \tag{8}$$

For convenience, stresses and strains are split into in-plane and out-of-plane components:

$$\sigma_p^{kT}=\begin{bmatrix}\sigma_1 & \sigma_2 & \sigma_6\end{bmatrix}^k,\sigma_n^{kT}=\begin{bmatrix}\sigma_5 & \sigma_4 & \sigma_3\end{bmatrix}^k; \tag{9}$$

$$\varepsilon_p^{kT} = \begin{bmatrix} \varepsilon_1 & \varepsilon_2 & \varepsilon_6 \end{bmatrix}^k, \varepsilon_n^{kT} = \begin{bmatrix} \varepsilon_5 & \varepsilon_4 & \varepsilon_3 \end{bmatrix}^k; \tag{10}$$

As a consequence the constitutive equations can be written,

$$\begin{aligned} \sigma_p^k &= \mathbf{C}_{pp}^k \varepsilon_p^k + \mathbf{C}_{pn}^k \varepsilon_n^k - \mathbf{e}_p^{k\,T} \mathbf{E}^k - \mathbf{q}_p^{k\,T} \mathbf{H}^k \\ \sigma_n^k &= \mathbf{C}_{pn}^{k\,T} \varepsilon_p^k + \mathbf{C}_{nn}^k \varepsilon_n^k - \mathbf{e}_n^{k\,T} \mathbf{E}^k - \mathbf{q}_n^{k\,T} \mathbf{H}^k \\ \mathbf{D}^k &= \mathbf{e}_p^k \varepsilon_p^k + \mathbf{e}_n^k \varepsilon_n^k + \varepsilon^k \mathbf{E}^k + \mathbf{d}^k \mathbf{H}^k \\ \mathbf{B}^k &= \mathbf{q}_p^k \varepsilon_p^k + \mathbf{q}_n^k \varepsilon_n^k + \mathbf{d}^k \mathbf{E}^k + \mu^k \mathbf{H}^k \end{aligned} \tag{11}$$

The explicit form of the introduced matrices follows:

$$\mathbf{C}_{pp}^k = \begin{bmatrix} C_{11} & C_{12} & C_{16} \\ C_{12} & C_{22} & C_{26} \\ C_{16} & C_{26} & C_{66} \end{bmatrix}^k, \mathbf{C}_{pn}^k = \begin{bmatrix} 0 & 0 & C_{13} \\ 0 & 0 & C_{23} \\ 0 & 0 & C_{36} \end{bmatrix}^k, \mathbf{C}_{nn}^k = \begin{bmatrix} C_{55} & C_{45} & 0 \\ C_{45} & C_{44} & 0 \\ 0 & 0 & C_{33} \end{bmatrix}^k; \tag{12}$$

$$\mathbf{e}_p^k = \begin{bmatrix} 0 & 0 & 0 \\ 0 & 0 & 0 \\ e_{31} & e_{32} & e_{33} \end{bmatrix}^k, \mathbf{e}_n^k = \begin{bmatrix} e_{15} & e_{14} & 0 \\ e_{25} & e_{24} & 0 \\ 0 & 0 & e_{36} \end{bmatrix}^k, \varepsilon^k = \begin{bmatrix} \varepsilon_{11} & \varepsilon_{12} & 0 \\ \varepsilon_{12} & \varepsilon_{22} & 0 \\ 0 & 0 & \varepsilon_{33} \end{bmatrix}^k; \tag{13}$$

$$\mathbf{q}_p^k = \begin{bmatrix} 0 & 0 & 0 \\ 0 & 0 & 0 \\ q_{31} & q_{32} & q_{33} \end{bmatrix}^k, \mathbf{q}_n^k = \begin{bmatrix} q_{15} & q_{14} & 0 \\ q_{25} & q_{24} & 0 \\ 0 & 0 & q_{33} \end{bmatrix}^k, \mu^k = \begin{bmatrix} \mu_{11} & \mu_{12} & 0 \\ \mu_{12} & \mu_{22} & 0 \\ 0 & 0 & \mu_{33} \end{bmatrix}^k; \tag{14}$$

$$\mathbf{d}^k = \begin{bmatrix} d_{11} & d_{12} & 0 \\ d_{12} & d_{22} & 0 \\ 0 & 0 & d_{33} \end{bmatrix}^k \tag{15}$$

$$\mathbf{E}^{kT} = \begin{bmatrix} E_1 & E_2 & E_3 \end{bmatrix}^k, \mathbf{D}^{kT} = \begin{bmatrix} D_1 & D_2 & D_3 \end{bmatrix}^k. \tag{16}$$

$$\mathbf{H}^{kT} = \begin{bmatrix} H_1 & H_2 & H_3 \end{bmatrix}^k, \mathbf{B}^{kT} = \begin{bmatrix} B_1 & B_2 & B_3 \end{bmatrix}^k. \tag{17}$$

2.2 Geometric relations

Strain-displacement relations in the linear case are:

$$\varepsilon_{pG}^k = \mathbf{D}_p \mathbf{u}^k, \varepsilon_{nG}^k = (\mathbf{D}_{np} + \mathbf{D}_{nz})\mathbf{u}^k, \tag{18}$$

where $\mathbf{u}^k$ is the vector of the displacement components:

$$\mathbf{u}^{kT} = \begin{bmatrix} u_x & u_y & u_z \end{bmatrix}^k. \tag{19}$$

The explicit forms of the differential matrices are:

$$\mathbf{D}_p = \begin{bmatrix} \partial_x & 0 & 0 \\ 0 & \partial_y & 0 \\ \partial_y & \partial_x & 0 \end{bmatrix}, \mathbf{D}_{np} = \begin{bmatrix} 0 & 0 & \partial_x \\ 0 & 0 & \partial_y \\ 0 & 0 & 0 \end{bmatrix}, \mathbf{D}_{nz} = \begin{bmatrix} \partial_z & 0 & 0 \\ 0 & \partial_z & 0 \\ 0 & 0 & \partial_z \end{bmatrix}. \quad (20)$$

The electric field $\mathbf{E}$ is related to the electric potential by the following gradient relation:

$$\mathbf{E}^{kT} = \begin{bmatrix} -\partial_x & -\partial_y & -\partial_z \end{bmatrix} \mathbf{\Phi}^k . \quad (21)$$

Being the electric potential $\mathbf{\Phi}$ a scalar, one has:

$$\mathbf{E}^k = (\mathbf{D}_{ep} + \mathbf{D}_{ez}) \mathbf{\Phi}^k , \quad (22)$$

where:

$$\mathbf{D}_{ep}^T = \begin{bmatrix} -\partial_x & -\partial_y & 0 \end{bmatrix}, \mathbf{D}_{ez}^T = \begin{bmatrix} 0 & 0 & -\partial_z \end{bmatrix}. \quad (23)$$

The magnetic field $\mathbf{H}$ is related to the magnetic potential by the following gradient relation:

$$\mathbf{H}^{kT} = \begin{bmatrix} -\partial_x & -\partial_y & -\partial_z \end{bmatrix} \mathbf{\Psi}^k . \quad (24)$$

Being the magnetic potential $\mathbf{\Psi}$ a scalar, one has:

$$\mathbf{H}^k = (\mathbf{D}_{hp} + \mathbf{D}_{hz}) \mathbf{\Psi}^k \quad , \quad (25)$$

where:

$$\mathbf{D}_{hp}^T = \begin{bmatrix} -\partial_x & -\partial_y & 0 \end{bmatrix}, \mathbf{D}_{hz}^T = \begin{bmatrix} 0 & 0 & -\partial_z \end{bmatrix}. \quad (26)$$

3. Extended Principle of Virtual Displacements for magneto-electro-elastic problems

It is of interest to present a full derivation of the extension of PVD to MEE continua by starting from the Hamilton's principle:

$$\delta \int_{t_0}^{t} (K - \Pi)\, dt = 0 \Rightarrow \delta \int_{t_0}^{t} K dt - \delta \int_{t_0}^{t} \Pi dt = 0 , \quad (27)$$

where K is the kinetic energy and Π is the potential energy.

The kinetic energy variation can be written:

$$\begin{aligned} \delta \int_{t_0}^{t} K\, dt &= \delta \int_{t_0}^{t} dt \int_V (\frac{1}{2} \rho \dot{u} \dot{u})\, dV = \int_{t_0}^{t} \int_V \rho \dot{u}\, \delta \dot{u}\, dV\, dt \\ &= \int_V \rho \dot{u}_i \delta u_i\, dV \Big|_{t_0}^{t_1} - \int_{t_0}^{t_1} \int_V \rho u_i\, \delta u_i\, dV\, dt \end{aligned} . \quad (28)$$

δu is equal zero in $t = t_0$ e $t = t_1$ then, the kinetic energy is:

$$\delta \int_{t_0}^{t} K\, dt = -\int_{t_0}^{t_1} \int_V \rho u_i\, \delta u_i\, dV\, dt \quad (29)$$

and

$$\delta \int_{t_0}^{t} K\, dt = -\int_{t_0}^{t} \delta L_{in} dt . \quad (30)$$

The potential energy variation can be written as in the following:

$$\delta\int_{t_0}^{t}\Pi dt = \delta\int_{t_0}^{t}\left[\int_V G_2(\varepsilon_{ij},E_i,H_i)\,dV - \int_\Omega\left(\bar{t}_j u_j - \bar{Q}\Phi - \bar{R}\Psi\right)d\Omega\right]dt$$
$$= \delta\int_{t_0}^{t}\int_V G_2(\varepsilon_{ij},E_i,H_i)\,dVdt - \delta\int_{t_0}^{t}\int_\Omega\left(\bar{t}_j u_j - \bar{Q}\Phi - \bar{R}\Psi\right)d\Omega dt \quad (31)$$
$$= \delta\int_{t_0}^{t}\int_V G_2(\varepsilon_{ij},E_i,H_i)\,dVdt - \int_{t_0}^{t}\delta L_e dt$$

where:
V is the plate volume;
Ω is the plate area;
$\bar{t}_j$ is the load in j-direction;
$\bar{Q}$ is the electric charge density on the plate surface;
$\bar{R}$ is the magnetic charge density on the plate surface;
Φ is the electric potential;
Ψ is the magnetic potential;
G_2 magnetoelectric Gibbs energy.

Upon substitution of Eqns.(31) and (30) in Eqn.(27) it follows:

$$-\int_{t_0}^{t}\delta L_{in}dt - \delta\int_{t_0}^{t}\int_V G_2(\varepsilon_{ij},E_i,H_i)\,dVdt + \int_{t_0}^{t}\delta L_e dt = 0 \quad (32)$$

and

$$\delta\int_{t_0}^{t}\int_V G_2(\varepsilon_{ij},E_i,H_i)\,dVdt = +\int_{t_0}^{t}\delta L_e dt - \int_{t_0}^{t}\delta L_{in}dt\,. \quad (33)$$

The subscript G will be used to denote those terms computed through the geometric relations and the subscript C to denote the ones that are calculated through the constitutive relations.

The variation of Gibbs energy holds:

$$\delta\int_{t_0}^{t}\int_V G(\varepsilon_{ij},E_i,H_i)dV\,dt$$
$$= \int_{t_0}^{t}\int_V\left(\frac{\partial G}{\partial\varepsilon_{ij}}\delta\varepsilon_{ij} + \frac{\partial G}{\partial E_i}\delta E_i + \frac{\partial G}{\partial H_i}\delta H_i\right)dV\,dt\,. \quad (34)$$

Taking into account Eqn. (4) we obtain:

$$\delta\int_{t_0}^{t}\int_V G(\varepsilon_{ij},E_i,H_i)\,dV\,dt = \int_{t_0}^{t}\int_V(\sigma_{ij}\,\delta\varepsilon_{ij} - D_i\,\delta E_i - B_i\,\delta H_i)dV\,dt\,. \quad (35)$$

By taking into account Eqns. (29), (30), (31) and by introducing these last in Eqn. (35) it follows that:

$$\int_{t_0}^{t}\int_V(\sigma_{ij}\,\delta\varepsilon_{ij} - D_i\,\delta E_i - B_i\,\delta H_i)\,dVdt = \int_{t_0}^{t}\delta L_e\,dt - \int_{t_0}^{t}\int_V\rho\,\ddot{u}_j\,\delta u_j\,dV\,dt \quad (36)$$

$$\int_{t_0}^{t}\int_V(\sigma_{ij}\delta\varepsilon_{ij} - D_i\delta E_i - B_i\delta H_i)dV\,dt = \int_{t_0}^{t}\int_V\delta L_e dt - \int_{t_0}^{t}\delta L_{in}dt\,. \quad (37)$$

Upon introducing the multilayered plate notations and by eliminating the time integral, the following variational statement is obtained:

$$\sum_{k=1}^{N_l} \int_{\Omega_k} \int_{h_k} \left\{ \delta\varepsilon_{pG}^{k\ T} \sigma_{pC}^k + \delta\varepsilon_{nG}^{k\ T} \sigma_{nC}^k - \delta \mathbf{E}_G^{k\ T} \mathbf{D}_C^k - \delta \mathbf{H}_G^{k\ T} \mathbf{B}_C^k \right\} d\Omega_k dz = \delta L_e - \delta L_{in} \quad (38)$$

which is the desired extension of the Principle of Virtual Displacements to a MEE continua. In [6] such a variational statement has been stated as PVD-6.

4. Unified Formulation for Plate Elements

The UF consists of a technique which permits to handle in a unified manner a large variety of plate modelings. This is made by expressing governing equations and/or finite element matrices in term of a few fundamental nuclei which do not formally depend on: - expansion N used in the z -direction; - number of nodes N_n of the element; - variables description (LW or ESL).

In MEE problems the unknown variables are the displacements, the electric potential and the magnetic potential. The following 'axiomatic' expansion is used for displacements:

$$\mathbf{u}^k(x,y,z) = F_b(z)\mathbf{u}_b^k(x,y) + F_r(z)\mathbf{u}_r^k(x,y) + F_t(z)\mathbf{u}_t^k(x,y) \quad r = 2,\ldots,N \quad (39)$$

or in compact form:

$$\mathbf{u}^k(x,y,z) = F_s\, \mathbf{u}_s^k . \quad (40)$$

$F_s(z)$ are function of the thickness coordinate z which can assume different forms. $\mathbf{u}_s$ are the two-dimensional 2D unknowns. Electric and magnetic potentials are assumed as the displacements:

$$\phi^k(x,y,z) = F_b(z)\phi_b^k(x,y) + F_r(z)\phi_r^k(x,y) + F_t(z)\phi_t^k(x,y) \quad r = 2,\ldots,N \quad (41)$$

$$\psi^k(x,y,z) = F_b(z)\psi_b^k(x,y) + F_r(z)\psi_r^k(x,y) + F_t(z)\psi_t^k(x,y) \quad r = 2,\ldots,N \quad (42)$$

or in compact form:

$$\phi^k(x,y,z) = F_s\, \phi_s^k \quad (43)$$

$$\psi^k(x,y,z) = F_s\, \psi_s^k . \quad (44)$$

Thickness functions could be the same for the three assumed fields. Of course this is not mandatory and in same cases it could be not convenient.

4.1 Equivalent Single Layer Model, ESLM

The above assumption can be used at layer or at multilayer level: LW and ESL theories are obtained, respectively. Depending on the made choice for the polynomials $F(z)$ a large variety of plate modelings can be introduced. In the ESL case the laminate is treated as a single layer. The subscript k, is therefore omitted. A first natural choice for thickness functions $F(z)$ consist to refer to power of z polynomials:

$$F_b = 1, \quad F_r = z^r, \quad F_t = z^N \quad r = 2,\ldots,N-1 . \quad (45)$$

That is a Taylor-type expansion is used and the variables related to F_b corresponds to the middle plane values; higher-order terms correspond instead to higher order derivatives calculated with correspondence to the reference surface of the plate. These ESL plate elements will be denote by the acronyms EDN in which: E means ESL, D states that PVD has been employed, N ranges from 1 to 4 to denote the order of the Taylor expansion.

4.2 Layer Wise Model, LWM

If a detailed response of individual layers is required and if significant variations in gradients between layers exist, LWM must be referred to. Each layer is seen as an independent layer and the continuity of the field variables at the interfaces is imposed as a constraint. The use of Taylor type expansion in each layer is not convenient. Top-bottom continuity would require additional conditions on the field variables. In order to avoid this drawback an appropriate combination of Legendre's Polynomials could be conveniently used as base function according to the following:

$$F_t = \frac{P_0 + P_1}{2}, \quad F_b = \frac{P_0 - P_1}{2}, \quad F_r = P_r - P_{r-2} \quad r = 2,\ldots,N \tag{46}$$

Where $P_i(\zeta_k)$ is the i-th-order Legendre polynomial in the domain $-1 \le \zeta_k \le 1$. The first five Legendre polynomials are:

$$P_0 = 1,\ P_1 = \zeta_k,\ P_2 = \frac{3\zeta^2 - 1}{2},\ P_3 = \frac{5\zeta^3 - 3\zeta}{2},\ P_4 = \frac{35\zeta^4 - 30\zeta^2 + 3}{8} \tag{47}$$

The chosen functions have the following properties:

$$\zeta_k = \begin{cases} 1: & F_t = 1, \quad F_b = 0, \quad F_r = 0 \\ -1: & F_t = 0, \quad F_b = 1, \quad F_r = 0 \end{cases} \tag{48}$$

For instance, in case of displacements variables, $\mathbf{u}_t^k$ e $\mathbf{u}_b^k$ are the top and bottom displacement of the k^{th} layer; the continuity condition is therefore easily written as:

$$\mathbf{u}_t^k = \mathbf{u}_b^{(k+1)}, \quad \text{with} \quad k = 1,\ldots,N_L - 1 \tag{49}$$

In this work electric potential and transverse stresses are described as LW variables. As in the ESL cases, plate element corresponding to LW description will be denoted by LDN acronyms.

4.3 Finite Element Approximations

Finite element approximations into the plate reference surface domain are introduced by means of iso-parametric descriptions for the various field variables.

$$\mathbf{u}_s^k(x,y) = N_j \mathbf{q}_{sj}^k \quad j = 1,2,\ldots,N_n \tag{50}$$

$$\mathbf{\Phi}_s^k(x,y) = N_j g_{sj}^k \quad j = 1,2,\ldots,N_n \tag{51}$$

$$\mathbf{\Psi}_s^k(x,y) = N_j b_{sj}^k \quad j = 1,2,\ldots,N_n \tag{52}$$

$N_j = N_j(x, y)$ are the shape functions, $\mathbf{q}_{sj}^k$ are the nodal unknown displacements, g_{sj}^k is the nodal unknown electric potential, b_{sj}^k is the nodal unknown magnetic potential.

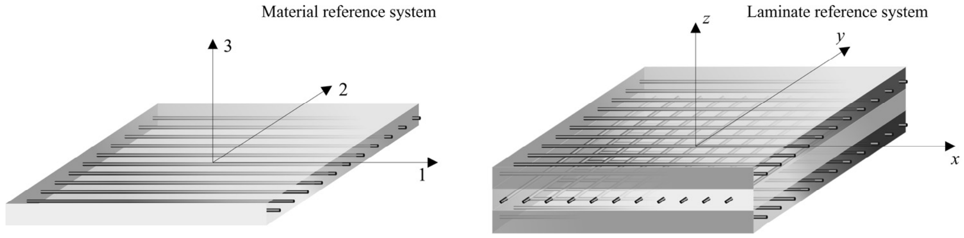

Fig.1 Geometry and notation for multilayered plates.

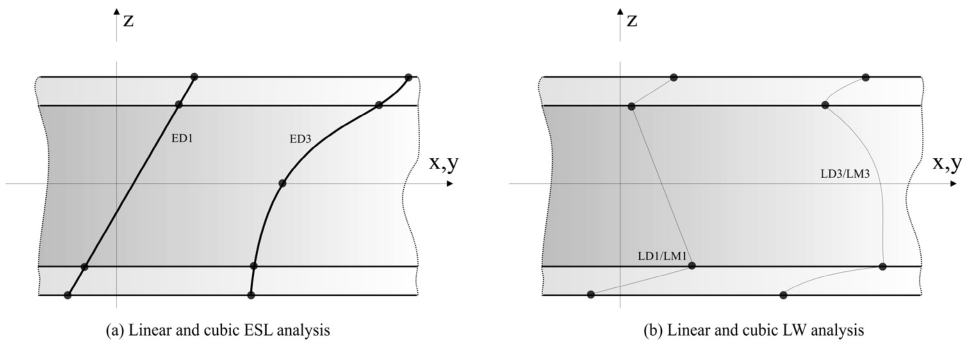

Fig.2 Examples of displacement fields related to some particular-case theories.

Substituting Eq. (50) in Eq. (40) we obtain:

$$\mathbf{u}^k(x, y, z) = F_s\, N_j\, \mathbf{q}_{sj}^k\,. \tag{53}$$

Substituting Eq. (51) in Eq. (43) we obtain:

$$\Phi^k(x, y, z) = F_s\, N_j\, g_{sj}^k\,. \tag{54}$$

Substituting Eq. (52) in Eq. (44) we obtain:

$$\Psi^k(x, y, z) = F_s\, N_j\, b_{sj}^k\,. \tag{55}$$

Quadrilater elements have been developed in this work and nine nodes Q9 elements are mostly considered in the numerical investigation.

4.3.1 Derivation of FE matrices for magneto-electro-elastic plates

By starting from Eq.(38), the fundamental nuclei of various finite element matrices related to PVD applications are obtained according to the following five steps:

1. The constitutive relations Eq.(11) are introduced in the PVD Eq.(38);
2. The geometric relations Eqs.(18),(22) and (25) are used to express strains in terms of displacements and electric and magnetic fields in terms of their potentials;

3. The through-the-thickness assumptions by means of the UF are introduced , see Eqn. (40), (43), (44);
4. FE shape functions Eqs.(50), (51) and (52) are used to integrate the in-plane plate coordinates;
5. Matrix products are made and explicit forms of fundamental nuclei of various FE matrices are obtained.

All the necessary steps are herein omitted for the sake of brevity. However the final form of governing equations is written as in the following:

$$\begin{aligned}
&\delta \mathbf{q}_{\tau i}^{k\,T} : \mathbf{K}_{uu}^{k\tau sij}\, \mathbf{q}_{sj}^{k} + \mathbf{K}_{ue}^{k\tau sij}\, g_{sj}^{k} + \mathbf{K}_{uh}^{k\tau sij}\, b_{sj}^{k} = \mathbf{P}_{u\tau}^{k} - \mathbf{M}_{u\ddot{u}}^{k\tau sij}\, \ddot{\mathbf{q}}_{sj}^{k} \\
&\delta g_{\tau i}^{k\,T} : \mathbf{K}_{eu}^{k\tau sij}\, \mathbf{q}_{sj}^{k} + \mathbf{K}_{ee}^{k\tau sij}\, g_{sj}^{k} + \mathbf{K}_{eh}^{k\tau sij}\, b_{sj}^{k} = \mathbf{P}_{e\tau}^{k} \qquad (56)\\
&\delta b_{\tau i}^{k\,T} : \mathbf{K}_{hu}^{k\tau sij}\, \mathbf{q}_{sj}^{k} + \mathbf{K}_{he}^{k\tau sij}\, g_{sj}^{k} + \mathbf{K}_{hh}^{k\tau sij}\, b_{sj}^{k} = \mathbf{P}_{h\tau}^{k}
\end{aligned}$$

Where the mechanical, electrical and magnetical loadings take the following form, respectively :

$$\mathbf{P}_{u\tau}^{k} = \mathbf{K}_{up}^{k\tau sij}\mathbf{p}_{sj} \qquad (57)$$

$$\mathbf{P}_{e\tau}^{k} = -\mathbf{K}_{ef}^{k\tau sij}\mathbf{\Phi}_{sj} \qquad (58)$$

$$\mathbf{P}_{h\tau}^{k} = -\mathbf{K}_{hf}^{k\tau sij}\mathbf{\Psi}_{sj} \qquad (59)$$

The equations (56) produce the final system of the governing FE matrix related to PVD applications. The following fundamental nuclei have been introduced:

$$\mathbf{K}_{uu}^{k\tau sij}, \mathbf{K}_{ue}^{k\tau sij}, \mathbf{K}_{uh}^{k\tau sij}, \mathbf{K}_{eu}^{k\tau sij}, \mathbf{K}_{ee}^{k\tau sij}, \mathbf{K}_{eh}^{k\tau sij}, \mathbf{K}_{hu}^{k\tau sij}, \mathbf{K}_{he}^{k\tau sij}, \mathbf{K}_{hh}^{k\tau sij}, \mathbf{K}_{ef}^{k\tau sij}, \mathbf{K}_{hf}^{k\tau sij}, \mathbf{K}_{up}^{k\tau sij}, \mathbf{M}_{u\ddot{u}}^{k\tau sij}.$$

The explicit array forms are:

$$\begin{aligned}
\mathbf{K}_{uu}^{k\tau sij} = \int_{\Omega_k} &[(\mathbf{D}_p^T N_i)(\mathbf{C}_{pp}^k E_{\tau s}^{uu} (\mathbf{D}_p N_j) + \mathbf{C}_{pn}^k E_{\tau s}^{uu} (\mathbf{D}_{np} N_j) + \mathbf{C}_{pn}^k E_{\tau s_{,z}}^{uu} N_j) \\
&+ (\mathbf{D}_{np}^T N_i)(\mathbf{C}_{pn}^{k\,T} E_{\tau s}^{uu} (\mathbf{D}_p N_j) + \mathbf{C}_{nn}^k E_{\tau s}^{uu} (\mathbf{D}_{np} N_j) + \mathbf{C}_{nn}^k E_{\tau s_{,z}}^{uu} N_j) \qquad (60)\\
&+ N_i (\mathbf{C}_{pn}^{k\,T} E_{\tau_{,z} s}^{uu} (\mathbf{D}_p N_j) + \mathbf{C}_{nn}^k E_{\tau_{,z} s}^{uu} (\mathbf{D}_{np} N_j) + \mathbf{C}_{nn}^k E_{\tau_{,z} s_{,z}}^{uu} N_j)]\, d\Omega_k
\end{aligned}$$

$$\begin{aligned}
\mathbf{K}_{ue}^{k\tau sij} = -\int_{\Omega_k} &[(\mathbf{D}_p^T N_i)\mathbf{e}_p^{k\,T}(E_{\tau s}^{ue} (\mathbf{D}_{ep} N_j) + E_{\tau s_{,z}}^{ue} (N_j I^*)) \\
&+ (\mathbf{D}_{np}^T N_i)\mathbf{e}_n^{k\,T}(E_{\tau s}^{ue} (\mathbf{D}_{ep} N_j) + E_{\tau s_{,z}}^{ue} (N_j I^*)) \qquad (61)\\
&+ N_i\, \mathbf{e}_n^{k\,T}(E_{\tau_{,z} s}^{ue} (\mathbf{D}_{ep} N_j) + E_{\tau_{,z} s_{,z}}^{ue} (N_j I^*))]\, d\Omega_k
\end{aligned}$$

$$\begin{aligned}
\mathbf{K}_{uh}^{k\tau sij} = -\int_{\Omega_k} &[(\mathbf{D}_p^T N_i)\mathbf{q}_p^{k\,T}(E_{\tau s}^{uh} (\mathbf{D}_{hp} N_j) + E_{\tau s_{,z}}^{uh} (N_j I^*)) \\
&+ (\mathbf{D}_{np}^T N_i)\mathbf{q}_n^{k\,T}(E_{\tau s}^{uh} (\mathbf{D}_{hp} N_j) + E_{\tau s_{,z}}^{uh} (N_j I^*)) \qquad (62)\\
&+ N_i\, \mathbf{q}_n^{k\,T}(E_{\tau_{,z} s}^{uh} (\mathbf{D}_{hp} N_j) + E_{\tau_{,z} s_{,z}}^{uh} (N_j I^*))]\, d\Omega_k
\end{aligned}$$

$$\begin{aligned}\mathbf{K}_{eu}^{k\tau sij} = -\int_{\Omega_k} [(\mathbf{D}_{ep}^T N_i)(\mathbf{e}_p^k E_{\tau s}^{eu} (\mathbf{D}_p N_j) + \mathbf{e}_n^k E_{\tau s}^{eu} (\mathbf{D}_{np} N_j) + \mathbf{e}_n^k E_{\tau s,_z}^{eu} N_j) \\ + (N_i I^*)^T (\mathbf{e}_p^k E_{\tau,_z s}^{eu} (\mathbf{D}_p N_j) + \mathbf{e}_n^k E_{\tau,_z s}^{eu} (\mathbf{D}_{np} N_j) + \mathbf{e}_n^k E_{\tau,_z s,_z}^{eu} N_j)] d\Omega_k\end{aligned} \tag{63}$$

$$\begin{aligned}\mathbf{K}_{ee}^{k\tau sij} = -\int_{\Omega_k} [(\mathbf{D}_{ep}^T N_i)\, \varepsilon^k (E_{\tau s}^{ee} (\mathbf{D}_{ep} N_j) + E_{\tau s,_z}^{ee} (N_j I^*)) \\ + (N_i \mathbf{I}^*)^T \varepsilon^k (E_{\tau,_z s}^{ee} (\mathbf{D}_{ep} N_j) + E_{\tau,_z s,_z}^{ee} (N_j I^*))] d\Omega_k\end{aligned} \tag{64}$$

$$\begin{aligned}\mathbf{K}_{eh}^{k\tau sij} = -\int_{\Omega_k} [(\mathbf{D}_{ep}^T N_i)\, \mathbf{d}^k (E_{\tau s}^{eh} (\mathbf{D}_{hp} N_j) + E_{\tau s,_z}^{eh} (N_j I^*)) \\ + (N_i \mathbf{I}^*)^T \mathbf{d}^k (E_{\tau,_z s}^{eh} (\mathbf{D}_{hp} N_j) + E_{\tau,_z s,_z}^{eh} (N_j I^*))] d\Omega_k\end{aligned} \tag{65}$$

$$\begin{aligned}\mathbf{K}_{hu}^{k\tau sij} = -\int_{\Omega_k} [(\mathbf{D}_{hp}^T N_i)(\mathbf{q}_p^k E_{\tau s}^{hu} (\mathbf{D}_p N_j) + \mathbf{q}_n^k E_{\tau s}^{hu} (\mathbf{D}_{np} N_j) + \mathbf{q}_n^k E_{\tau s,_z}^{hu} N_j) \\ + (N_i I^*)^T (\mathbf{q}_p^k E_{\tau,_z s}^{hu} (\mathbf{D}_p N_j) + \mathbf{q}_n^k E_{\tau,_z s}^{hu} (\mathbf{D}_{np} N_j) + \mathbf{q}_n^k E_{\tau,_z s,_z}^{hu} N_j)] d\Omega_k\end{aligned} \tag{66}$$

$$\begin{aligned}\mathbf{K}_{he}^{k\tau sij} = -\int_{\Omega_k} [(\mathbf{D}_{hp}^T N_i)\, \mathbf{d}^k (E_{\tau s}^{he} (\mathbf{D}_{ep} N_j) + E_{\tau s,_z}^{he} (N_j I^*)) \\ + (N_i \mathbf{I}^*)^T \mathbf{d}^k (E_{\tau,_z s}^{he} (\mathbf{D}_{hp} N_j) + E_{\tau,_z s,_z}^{he} (N_j I^*))] d\Omega_k\end{aligned} \tag{67}$$

$$\begin{aligned}\mathbf{K}_{hh}^{k\tau sij} = -\int_{\Omega_k} [(\mathbf{D}_{hp}^T N_i)\, \mu^k (E_{\tau s}^{hh} (\mathbf{D}_{hp} N_j) + E_{\tau s,_z}^{hh} (N_j I^*)) \\ + (N_i \mathbf{I}^*)^T \mu^k (E_{\tau,_z s}^{hh} (\mathbf{D}_{hp} N_j) + E_{\tau,_z s,_z}^{hh} (N_j I^*))] d\Omega_k\end{aligned} \tag{68}$$

$$\mathbf{K}_{up}^{k\tau sij} = \int_{\Omega_k} F_\tau^1 (N_i N_j \mathbf{m}_s^k) F_s^1 \; d\Omega_k \tag{69}$$

$$\mathbf{K}_{ef}^{k\tau sij} = \int_{\Omega_k} F_\tau^1 (N_i N_j n_s^k) F_s^1 \; d\Omega_k \tag{70}$$

$$\mathbf{K}_{hf}^{k\tau sij} = \int_{\Omega_k} F_\tau^1 (N_i N_j r_s^k) F_s^1 \; d\Omega_k \tag{71}$$

$$\mathbf{M}_{u\ddot{u}}^{k\tau sij} = \int_{\Omega_k} \rho^k (N_i \mathbf{I}) E_{\tau s}^{uu} (N_j \mathbf{I}) d\Omega_k \tag{72}$$

A_k and Ω_k indicate the *k*-th layer thickness and the surface respectively. $\mathbf{I}$ is the unit matrix and $\mathbf{I}^{\star T} = \{0, 0, -1\}$. The following integrals have been defined:

$$E_{\tau s}^{\alpha\beta} = \int_{A_k} F_\tau^\alpha F_s^\beta \; dz, \quad E_{\tau,_z s}^{\alpha\beta} = \int_{A_k} F_{\tau,_z}^\alpha F_s^\beta \; dz, \quad E_{\tau s,_z}^{\alpha\beta} = \int_{A_k} F_\tau^\alpha F_{s,_z}^\beta \; dz$$

where α and β can assume any of the values u, σ, B, D to denote thickness functions used for the related variables. Tab. 1 summarizes the dimensions of the fundamental nuclei. The explicit, scalar form of the fundamental nuclei can be seen in Appendix. The assembling procedure of the matrices for the different layers and different nodes is required to get the complete element matrices. The same techniques already used for the pure mechanical case have been referred to; see [23] for details.

4.3.2 Numerical Results

This section shows some numerical results to assess the developed FEs for static magneto-electrical-mechanical plate problems which are based on PVD application. Reduced integration techniques have been preserved as done in [9], [25], [26] and [27], to overcome locking phenomena.

Present FE analysis has been compared with 3D exact MEE solution by Pan [11]. Additional analysis are made by referring to the work by Lage et alii [18]. Square plates with simply supported edges are analyzed which are loaded at the top layer surface. Layered plates are build by using a combination of layers made of piezoelectric and magnetostrictive materials. The piezoelectric material consists of $BaTiO_3$ (called B for brevity) and the magnetostrictive one $CoFe_2O_4$ (called F for brevity). The physical properties of these two materials are given in Table 2 where C_{ij} , e_{ij} , q_{ij} are the stiffness, piezoelectric and piezo-magnetic coefficients, while p_{ij} and ν_{ij} are electric and magnetic permeability. The considered stacking sequences are B/F/B and F/B/F, the load is of bi-sinusoidal type; layer thickness is $h_k = 0.1$, plate length is $a = 1$ and whole given variables have been calculated with correspondence to the in-plane coordinate values: $x = 0.75$ and $y = 0.25$, as done in the referenced articles.

Quite comprehensive results are presented in Figs. 3, 4, 5 and 6: LW and ESL approaches are compared; B/F/B and F/B/F and MEE plates are considered; through-the-thickness distribution of mechanical, electrical and magnetical variables have been traced. Dots represent values in [18]. To notice that there are some differences between present solutions and those in [18]. These are due to the use of different mesh (we use 4×4 elements instead of 3×3 mesh in [18]); furthermore a short circuit boundary condition at the top and bottom plate surfaces has been considered in the present analysis, that condition has not been enforced in [18]. As a consequence of these last differences, the behaviors of the magnetic and electric potential of the present analysis are shifted with respect to that in [18]. Unfortunately, no additional results are available for this problem in the open literature.

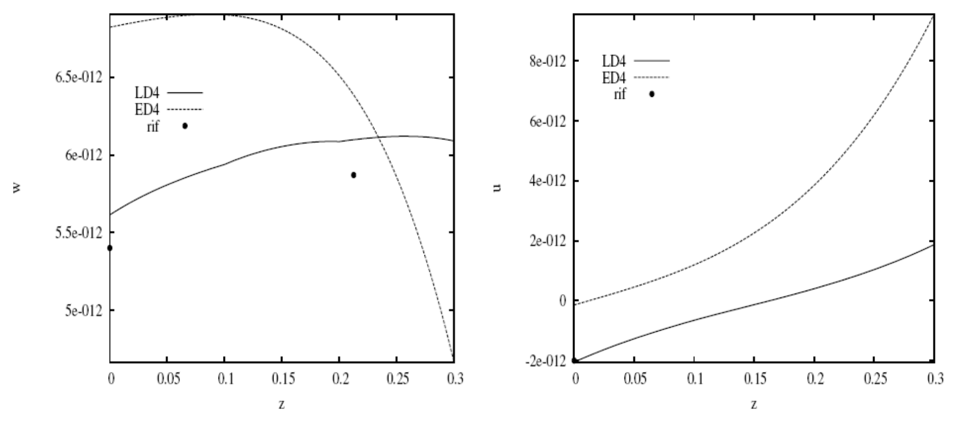

(a) Behavior along the thickness of transverse displacement displacement $w = u_z$

(b) Behavior along the thickness of the in-plane displacement $u = u_x$.

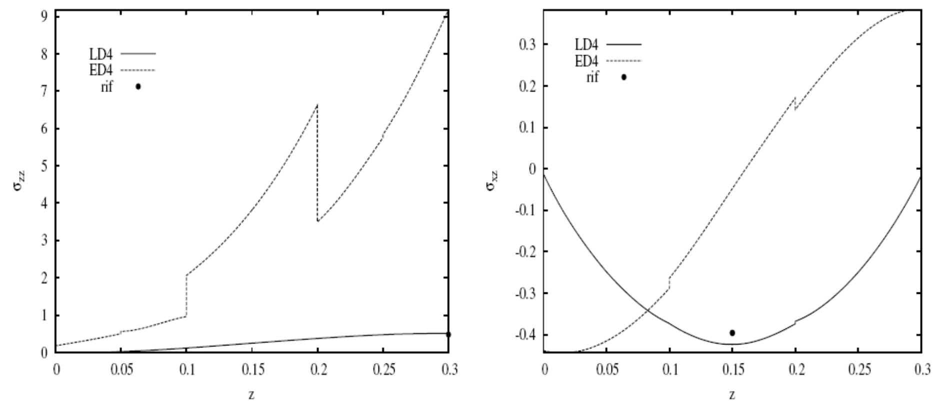

(c) Behavior along the thickness of the transverse normal stress σ_{zz}.
(d) Behavior along the thickness of tranverse shear stress σ_{xz}.

Fig.3. Through-the-thickness distribution of relevant variables for B/F/B plate. Comparison between LW and ESL analyses. The dots denoted as 'rif.' are the values from [18].

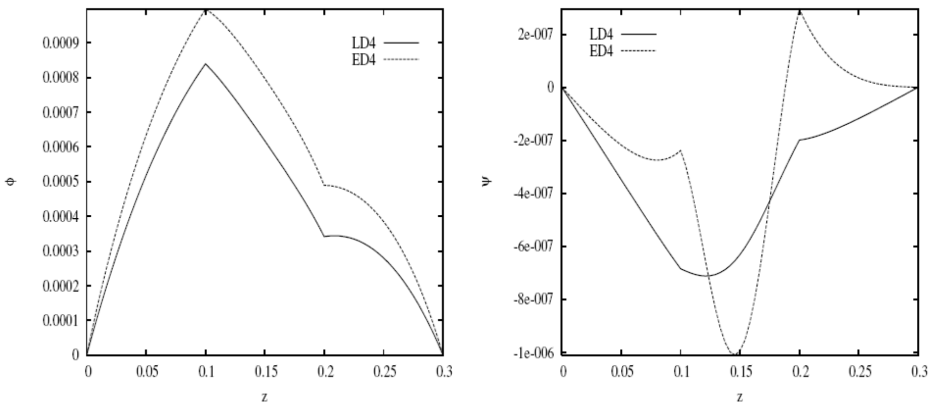

(a) Behavior along the thickness of the electric potential Φ
(b) Behavior along the thickness of the magnetic potential Ψ

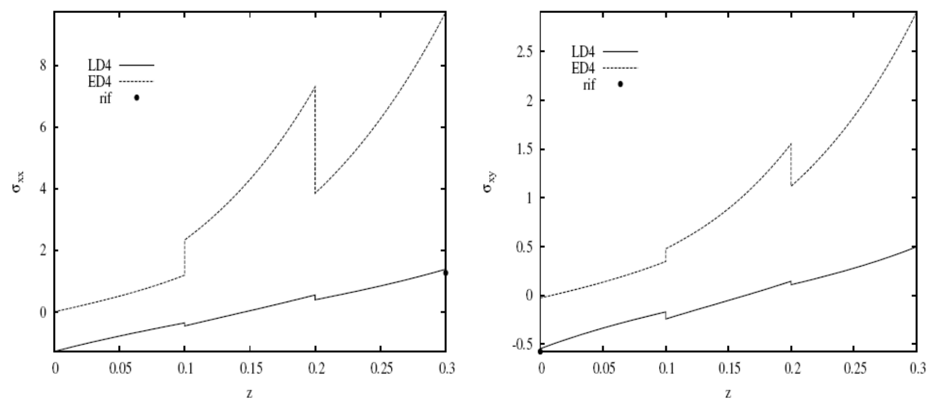

(c) Behavior along the thickness of the σ_{xx} tension and reference value (point)
(d) Behavior along the thickness of the σ_{xy} tension and reference value

Fig.4. Through-the-thickness distribution of relevant variables for B/F/B plate. Comparison between LW and ESL analyses. The dots denoted as 'rif.' are the values from [18].

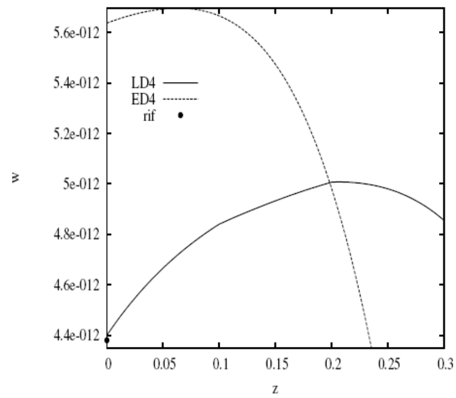

(a) Behavior along the thickness of the displacement $w = u_z$ and reference value (point)

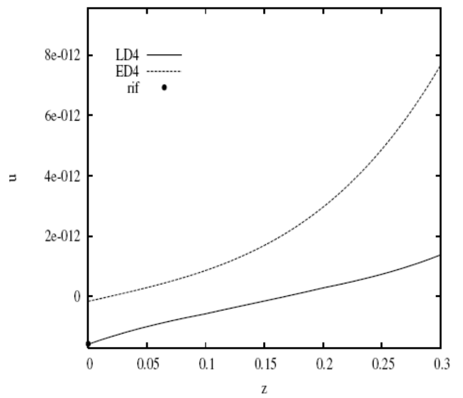

(b) Behavior along the thickness of the displacement $u = u_x$ and reference value

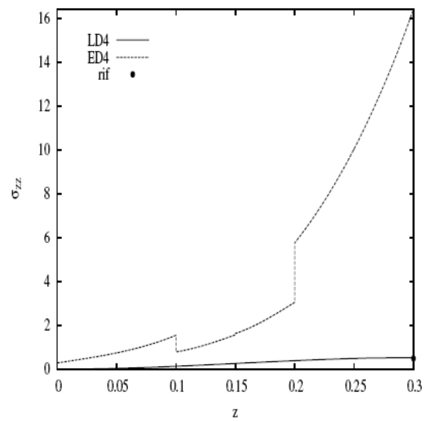

(c) Behavior along the thickness of the σ_{zz} tension and reference value

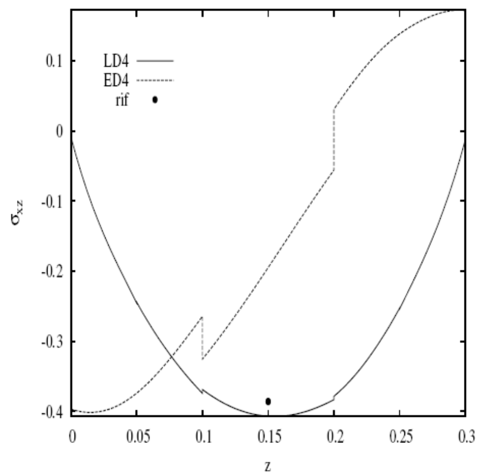

(d) Behavior along the thickness of the σ_{xz} tension and reference value

Fig.5. As Fig 3 for F/B/F plate.

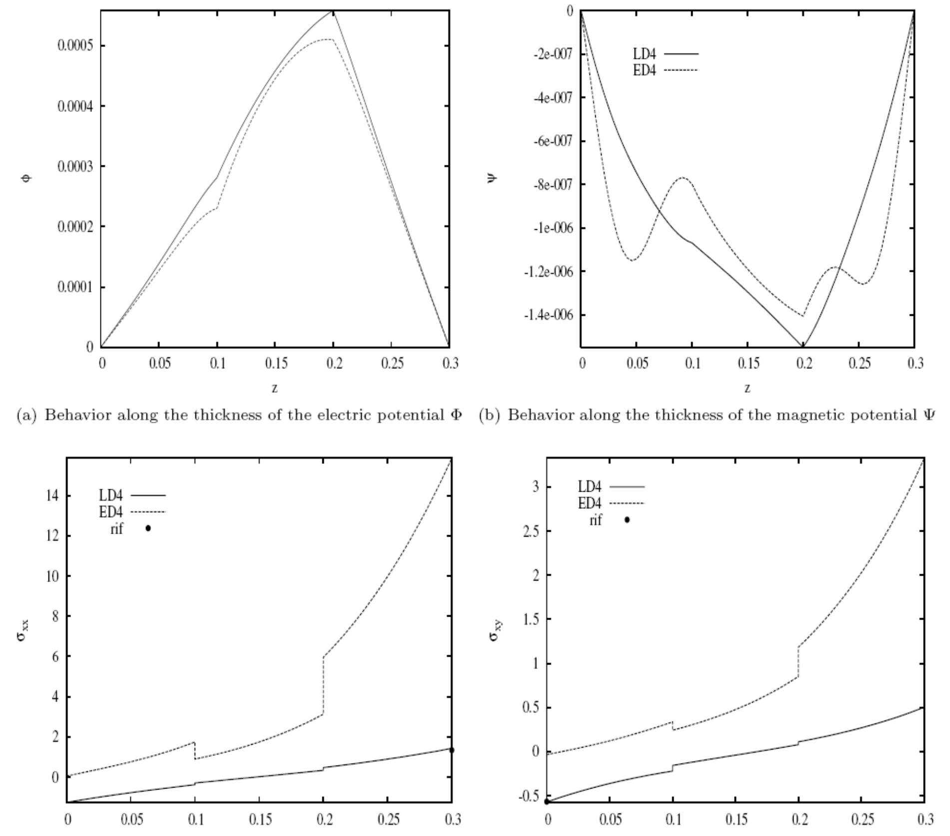

(a) Behavior along the thickness of the electric potential Φ (b) Behavior along the thickness of the magnetic potential Ψ

(c) Behavior along the thickness of the σ_{xx} tension and reference value (point) (d) Behavior along the thickness of the σ_{xy} tension and reference value

Fig.6. As Fig 4 for F/B/F plate.

Table 1. Dimensions of the fundamental nuclei.

Fundamental Nuclei	Dimension	Fundamental Nuclei	Dimension
$\mathbf{K}_{uu}^{k\tau sij}$	[3×3]	$\mathbf{K}_{hu}^{k\tau sij}$	[1×3]
$\mathbf{K}_{ue}^{k\tau sij}$	[3×1]	$\mathbf{K}_{he}^{k\tau sij}$	[1×1]
$\mathbf{K}_{uh}^{k\tau sij}$	[3×1]	$\mathbf{K}_{hh}^{k\tau sij}$	[1×1]
$\mathbf{K}_{eu}^{k\tau sij}$	[1×3]	$\mathbf{K}_{hf}^{k\tau sij}$	[1×1]
$\mathbf{K}_{ee}^{k\tau sij}$	[1×1]	$\mathbf{K}_{up}^{k\tau sij}$	[3×3]
$\mathbf{K}_{eh}^{k\tau sij}$	[1×1]		
$\mathbf{K}_{ef}^{k\tau sij}$	[1×1]		
$\mathbf{M}_{u\ddot{u}}^{k\tau sij}$	[3×3]		

Table 2. Properties of the employed materials in the reference work.

Properties	$BaTiO_3$	$CoFe_2O_4$	Properties	$BaTiO_3$	$CoFe_2O_4$
C_{11} [GPa]	166	286	e_{31} [C/m^2]	-4.4	0
C_{22} [GPa]	166	286	e_{32} [C/m^2]	-4.4	0
C_{12} [GPa]	77	173	e_{33} [C/m^2]	18.6	0
C_{13} [GPa]	78	170.5	e_{24} [C/m^2]	11.6	0
C_{23} [GPa]	78	170.5	e_{15} [C/m^2]	11.6	0
C_{33} [GPa]	162	269.5	q_{31} [$N/(Am)$]	0	580.3
C_{44} [GPa]	43	45.3	q_{32} [$N/(Am)$]	0	580.3
C_{55} [GPa]	43	45.3	q_{33} [$N/(Am)$]	0	699.7
C_{66} [GPa]	44.5	56.5	q_{24} [$N/(Am)$]	0	550
			q_{15} [$N/(Am)$]	0	550
$p_{11}\times10^9$ [$C^2/(Nm^2)$]	11.2	0.08			
$p_{22}\times10^9$ [$C^2/(Nm^2)$]	11.2	0.08			
$p_{33}\times10^9$ [$C^2/(Nm^2)$]	12.6	0.093			
$\nu_{11}\times10^6$ [Ns^2/C^2]	5	-590			
$\nu_{22}\times10^6$ [Ns^2/C^2]	5	-590			
$\nu_{33}\times10^6$ [Ns^2/C^2]	10	157			

The strong limitation of ESL analyses are clearly shown for both displacement and stress evaluations. In particular ESL analysis leads to interlaminar discontinuous transverse shear and normal stresses. The error exhibited by ESL analyses are very much subordinate to the computed variables. That error is larger for mechanical variable evaluations. Anyway such a conclusion could not be extended to different plate problems.

Linear, parabolic, 3rd and 4th order LW and ESL plate elements have been compared in Tabs. 3, 4, 5 and 6. These tables strongly confirm the above made comments.

Table 3. Comparison of various kinematics for B/F/B plate. Evaluation of transverse stresses and displacements.

	$\sigma_{zz}[Pa]$	$\sigma_{xz}[Pa]$	$u=u_x[m]$	$w=u_z[m]$
	TOP	$\frac{z}{2}$	BOT	BOT
LD1	0.74	-4.14×10^{-1}	-2.02×10^{-12}	5.5×10^{-12}
LD2	0.57	-4.31×10^{-1}	-2.05×10^{-12}	5.6×10^{-12}
LD3	0.55	-4.24×10^{-1}	-2.05×10^{-12}	5.6×10^{-12}
LD4	0.51	-4.23×10^{-1}	-2.05×10^{-12}	5.6×10^{-12}
ED1	1.38	-1.94×10^{0}	-1.24×10^{-13}	5.7×10^{-12}
ED2	3.95	-3.04×10^{-1}	-1.50×10^{-13}	6.4×10^{-12}
ED3	2.96	-1.00×10^{0}	-1.44×10^{-13}	6.72×10^{-12}
ED4	9.18	-4.78×10^{-2}	-1.45×10^{-13}	6.82×10^{-12}
[11],[18]	0.5	-3.96×10^{-1}	-2.01×10^{-12}	5.4×10^{-12}

Table 4. Comparison of various kinematics for B/F/B plate. Evaluation of in-plane stressees and electric and magnetic potentials.

	$\phi_{MAX}[V]$	$\psi_{MAX}[C/s]$	$\sigma_{xx}[Pa]$	σ_{xy} [Pa]
			TOP	BOT
LD1	8.33×10^{-4}	-7.07×10^{-7}	1.43	-5.38×10^{-1}
LD2	8.39×10^{-4}	-7.15×10^{-7}	1.39	-5.47×10^{-1}
LD3	8.39×10^{-4}	-7.11×10^{-7}	1.38	-5.48×10^{-1}
LD4	8.39×10^{-4}	-7.12×10^{-7}	1.38	-5.48×10^{-1}
ED1	5.98×10^{-4}	-6.65×10^{-7}	2.67	-3.35×10^{-2}
ED2	1.01×10^{-3}	-8.22×10^{-7}	4.39	-3.06×10^{-2}
ED3	9.86×10^{-4}	-8.08×10^{-7}	5.76	-3.02×10^{-2}
ED4	9.97×10^{-4}	-1.01×10^{-6}	9.72	-2.65×10^{-2}
[11],[18]	1.54×10^{-3}	-2.61×10^{-6}	1.27	-5.77×10^{-1}

Table 5. As Tab.4 for F/B/F plate.

	$\sigma_{zz}[Pa]$	$\sigma_{xz}[Pa]$	$u=u_x[m]$	$w=u_z[m]$
	TOP	$\frac{z}{2}$	BOT	BOT
LD1	0.83	-3.97×10^{-1}	-1.55×10^{-12}	4.33×10^{-12}
LD2	0.53	-4.11×10^{-1}	-1.583×10^{-12}	4.40×10^{-12}
LD3	0.51	-4.06×10^{-1}	-1.584×10^{-12}	4.40×10^{-12}
LD4	0.51	-4.06×10^{-1}	-1.585×10^{-12}	4.40×10^{-12}
ED1	1.56	-1.25×10^{0}	-1.30×10^{-13}	4.00×10^{-12}
ED2	8.73	-3.22×10^{-1}	-1.57×10^{-13}	5.44×10^{-12}
ED3	3.91	-7.84×10^{-1}	-1.58×10^{-13}	5.56×10^{-12}
ED4	16.4	-1.95×10^{-1}	-1.59×10^{-13}	5.64×10^{-12}
[11],[18]	0.5	-3.86×10^{-1}	-1.57×10^{-12}	4.38×10^{-12}

Table 6. As Tab.4 for a F/B/F plate.

	$\phi_{MAX}[V]$	$\psi_{MAX}[C/s]$	$\sigma_{xx}[Pa]$	σ_{xy} [Pa]
			TOP	BOT
LD1	5.54×10^{-4}	-1.63×10^{-7}	1.6	-5.49×10^{-1}
LD2	5.56×10^{-4}	-1.53×10^{-7}	1.44	-5.74×10^{-1}
LD3	5.58×10^{-4}	-1.55×10^{-7}	1.42	-5.74×10^{-1}
LD4	5.58×10^{-4}	-1.55×10^{-7}	1.42	-5.74×10^{-1}
ED1	4.48×10^{-4}	-3.00×10^{-6}	2.65	-4.81×10^{-2}
ED2	4.84×10^{-4}	-1.90×10^{-6}	8.26	-4.18×10^{-2}
ED3	5.62×10^{-4}	-1.73×10^{-6}	6.89	-4.21×10^{-2}
ED4	5.10×10^{-4}	-1.41×10^{-6}	15.9	-3.61×10^{-2}
[11],[18]	2.30×10^{-3}	-1.88×10^{-6}	1.33	-5.69×10^{-1}

4.3.3 Concluding Remarks

The paper has extended the UF to finite element analysis of magneto-electro-elastic multilayered plates. Full coupling among the three fields has been retained. A few numerical results have shown the effectiveness of the made developments as well as the convenience of referring to UF for multi-fields problems analyses. Future works should enlarge the numerical analysis to include, different geometries and different loading conditions. The developed Finite Element models could be conveniently applied to many other problems involving multifield couplings. Developments direct to the extension of mixed methods that enforce ’a priori’ interlaminar continuity of relevant electrical and magnetical as well as mechanical variables would be also welcome.

Acknowledgements

This work has been carried out in the framework of STREP EU project CASSEM under contract NMP-CT-2005-013517. The partial support of European Space Agency (ESTEC-Contract No. 21082/06/NL/PA) as well as of Piedmont Regional Project E40 is also acknowledgments.

References:

[1]. Chopra I, *SPIE smart struct and mat conf SPIE*, 2717(1996)20.
[2]. Chopra I, AIAA *Journal*, 40(2002)2145.
[3]. Mindlin R D, *J. Appl. Phys.*, 23(1952)83.
[4]. Tiersten H F and Mindlin R D, *Forced Vibrations of Piezoelectric Crystal Plates*, 20(1961)107.
[5]. Ikeda T, *Fundamentals of piezoelectricity*, 1996.
[6]. Carrera E, Brischetto S, Nali P, *Mech. Adv. Mater. Struct.*, 15(2008)182.
[7]. Carrera E, *Appl. Mech. Rev.*, 56(2003)287.
[8]. Carrera E, Brischetto S, *Journal of Mechanics of Materials and Structures,* 2(2007)377.
[9]. Carrera E, Fagiano C, *Journal of Mechanics of Materials and Structures*, 2(2007)421.
[10]. Corke T C, Post M L, *AIAA paper*, (2004)2004.
[11]. Pan E, *J. Appl. Mech. Eng.*, 68(2001)608.
[12]. Pan E, Heyliger P R, *J. Sound Vib.*, 252(2002)429.
[13]. Wang X, Zhong Z, *Int. J. Eng. Sci.*, 41(2003)2429.
[14]. Aboudi J, *Smart Mater. Struct.*, 10(2001)867.
[15]. Buchanan G R, *J. Sound Vib.*, 268(2003)413.
[16]. Buchanan G R, *Composites B (Engineering)*, 35(2004)413.
[17]. Wang J, Chen L, Fang S, *Int. J. Solids Struct.,* 40(2003)1669.
[18]. Lage G R, Soares C M, Soares C A, Reddy J N, *Computers and Structures*, 76(2004)299.
[19]. Chen W Q, Lee K Y, *Int. J. Solids Struct.*, 33(2003)977.
[20]. Chen W Q, Lee K Y, Ding H J, *J. Sound Vib.*, 279(2005)237.
[21]. Chen J, Chen H, Pan E, Heylegher P R, *J. Sound Vib.*, in press, 2007.
[22]. Weller T, Licht C, *C.R., Mechanique*, 335(2007)201.
[23]. Carrera E, *Archives of Computational Methods in Engineering*, 10(2003)215.
[24]. Carrera E, Demasi L, *Int. J. Numer. Methods Eng.*, 55(2002)191.
[25]. Carrera E, Demasi L, *Int. J. Numer. Methods Eng.*, 55(2002)253.
[26]. Carrera E, Boscolo M, *Int. J. Numer. Methods Eng.*, 70(2007)253.
[27]. Carrera E, Boscolo M, Robaldo A, *Archives of Computational Method in Engineering*, in press, 2007.